Intrachain carrier transport in conjugated polymer with structural and chemical defects

Yi-Shiou Chen and Hsin-Fei Meng*
Institute of Physics, National Chiao Tung University, Hsinchu 300, Taiwan, Republic of China
(Received 22 January 2002; published 11 July 2002)

By calculating the phase shifts of the wave functions for the extended scattering states within tight-binding model for a poly (p-phenylene vinylene) chain with one conjugation defect, we obtain the exact transmission probability through the defect as a function of the carrier incident energy for the entire eight π bands. Cis-defect, sp^3 saturation, and oxidation are considered. The transmission increases rapidly from zero with the carrier kinetic energy, implying the conjugation breaks do not severely limit the intrachain charge transport under high electric field. Assuming an average conjugation length of 100 Å separated by cis-defects, the drift velocity is predicted to be as high as 10^3 m/s for field at 10^7 V/m, and over 10^5 m/s at 10^8 V/m.

DOI: 10.1103/PhysRevB.66.035202 PACS number(s): 72.80.Le, 72.10.−d, 72.20.Ht

The physics of conjugated polymers have advanced dramatically in the past decades.[1] However, partly due to the amorphous and defective nature of the material, the connection between microscopic models based on polaron motion in a perfect chain and the macroscopic transport properties of a film is not well established. Technologically, the low macroscopic mobility has been one of the greatest obstacles to the development of optical and electronic devices based on conjugated polymers.[2,3] For example, the polymer injection laser has been considered as unfeasible because the exciton gain is overwhelmed by the absorption induced by the large number of carriers caused by low mobility.[3] Interchain hopping is assumed to be the main bottleneck for the transport, especially in the sandwich structure where the electric field is basically perpendicular to the chain direction. The natural question is then whether the mobility can be significantly raised if the chains are aligned and the field is applied parallel to the chain. The answer is not obvious, because one might expect that the carriers are confined within the conjugation length l_c, whose average is only about 100 Å.[4–6]

In this work we show theoretically by tight-binding model that, while the low-energy carriers are confined in l_c, the transmission coefficient of a carrier through a conjugation defect is not necessarily small for large incident wave number k measured from the band edge. Cis-defect[4] (chain twist), sat-defect[4] (double bond saturation by two sp^3 groups), and oxidation(carbonyl defect) are studied(Fig. 1). For cis-defect, the transmission probability T is 0.7 when $k=0.11(\pi/a)$, corresponding to velocity 3.2×10^5 m/s and kinetic energy 0.04 eV. $a=6.5$ Å is the lattice constant. In terms of the electric field, the averaged T over carrier distribution is equal to 0.7 when $E=6\times10^7$ V/m. Sat-defect confines the carriers much more severely due to the insertion of two sp^3 groups. The carbonyl group is found to break the electron-hole symmetry and confines holes much more effectively than the electrons. In order to obtain the overall intrachain drift velocity v_d, the drift time within l_c determined by the bare drift velocity v_d^0, and the ''delay time'' at the conjugation defect have to be added. The calculation is divided into three field regimes separated by $E_1=4\times10^7$ V/m and $E_2=10^8$ V/m. In the low-field regime ($E<E_1$), polaron forms and v_d^0 is limited by the sound velocity v_s. In the intermediate field regime ($E_1<E<E_2$), the carrier is free from lattice distortion but k is concentrated near the band minimum. v_d^0 increases roughly linearly with E. In the high-field regime ($E>E_2$),k is distributed almost evenly in the first Brillouin zone (FBZ), and v_d^0 decreases with E as required by energy balance. The effect of the defects is more pronounced at lower field due to the large delay time. Cis-defects are assumed to be the dominant conjugation breaks,[4] because sat-defects and oxidation can be eliminated under proper synthesis conditions.[7] In the low-field regime with $l_c=100$ Å,v_d is 3×10^3 m/s at $E=1.1\times10^7$ V/m.[8] The corresponding mobility is seven orders of magnitude larger than the interchain mobility.[9] Simple estimate (see below) shows that net optical gain can be realized at such v_d for an active region of 1 μm wide. Device with aligned polymer chains and parallel injection is therefore predicted to be potentially suitable for polymer laser even with present defect density of about one per 15 repeat units.[4,6]

The tight-binding model for the π electrons of a poly (p-phenyline vinylene) (PPV) chain with one defect has been described elsewhere.[10] The σ bonds formed by the sp^2 orbitals lie in the x-y plane. The $2p_z$ orbitals of carbon and oxygen, sp^3 of carbon, and hydrogen $1s$ are involved in the π bands. The chemical structures and bonding of the defects are shown in Fig. 1. t, t_1 and t_2 are the off-diagonal resonance integrals for the carbon phenyl, single, and double bonds, respectively. The cis-defect is an exchange between the hydrogen atom and the phenyl ring connected to a vinyl double bond. The steric potential results in a 144° ring out-of-plane rotation[4] after the exchange. So the twisted single bound is reduced by a factor of cos(144°). For the carbonyl and sat-defects, the normal $2p_z$ conjugation is broken by the sp^3 saturation of one (carbonyl) or two (sat) carbon atom(s) on the backbone. Nevertheless, the π orbitals on the two sides of the defects are still connected through the hyperconjugation with the sp^3 orbitals of the saturated carbon atom. On the saturated carbon atom two of the four sp^3 orbitals form σ bonds with the neighboring carbon atoms and lie on the x-y plane, while the remaining two out-of-plane orbitals are in the $z>0$ and $z<0$ sides of the x-y plane. Hyperconjugation is due to the nonzero resonance integrals of these two sp^3 orbitals with the $2p_z$ or sp^3 orbitals on the neigh-

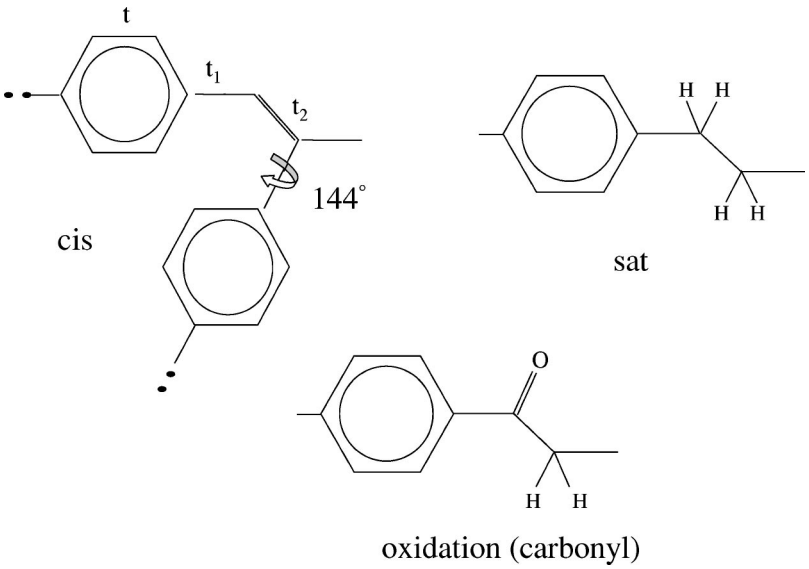

FIG. 1. The chemical structures of the three kinds of conjugation defects are shown. There is a 144° out-of-plane rotation for the cis-defect. The C—H bonds shown for the carbonyl and sat-defects are out-of-plane sp^3 orbitals.

boring carbon atoms. In addition, the oxygen $2p_z$ orbital and the $1s$ orbitals of the two hydrogen atoms bonded with the out-of-plane carbon sp^3 orbitals are also included in the tight-binding model due to the hyperconjugation. t_O is for C═O bond, t_H for *C—H* bond. $t_{h1}=\pm(t_1/2)\cos(\phi)$ is for carbon $2p_z$-sp^3 hyperconjugation.[11,12] $\phi=25.2°$ is the angle between the out-of-plane tetrahedral sp^3 orbital and the z direction. The $\pm$ signs are for the two sp^3 orbitals in the $z>0$ and $z<0$ sides of the x-y plane, respectively. $t_{h2}=t_1\cos(2\phi)$ is for sp^3-sp^3 hyperconjugation. The angle 2ϕ is because that the two sp^3 orbitals of one vinyl carbon atom are on the same side of the vertical plane, defined by the saturated double bond and the z axis, while the two orbitals of the other vinyl carbon atom are on the opposite side of the plane. The steric potential energy is minimized in such arrangement.[4] ε_O is the diagonal Coulomb integral for oxygen, ε_H is for hydrogen. They are relative to the carbon Coulomb integral, which is taken as zero. We choose $t=-3.1$ eV, $t_1=-2.2$ eV, $t_2=-3.0$ eV in order to reproduce the band structure obtained from *ab inito* calculation.[13] Other parameters used are $t_O=t_1$,[11] $t_H=-4$ eV,[14] $\varepsilon_O=t_1$,[11] and $\varepsilon_H=0$ (covalent bonding).

When a Bloch wave propagates toward a defect, it is partly transmitted and reflected. Our task is to obtain the scattering solution of the tight-binding Hamiltonian $|\pm k\rangle_s$, which is a purely transmitted wave on one side of the defect, and a superposition of the incident and reflected waves on the other side (see Fig. 2). $|k\rangle_s$ is incident from the left and $|-k\rangle_s$ from the right. k is chosen to be positive. $|\pm k\rangle$ denotes Bloch states in a perfect chain. So $|k\rangle_s=|k\rangle$ on the right side of the defect, while $|k\rangle_s=(1/t)|k\rangle+(r/t)|-k\rangle$ on the left side. The case for $|-k\rangle_s$ is the reverse. t and r are the complex transmission and reflection amplitudes. Their absolute squares T and $R(=1-T)$ are the transmission and reflection probabilities, respectively. In practice the tight-binding Hamiltonian is diagonalized in a finite but large ring with one defect. There are two nearly degenerate real eigenstates with different phase shifts across the defect at each energy inside the continuum, which can be labeled as $|k1\rangle$ and $|k2\rangle$ (Fig. 2). The scattering states $|k\rangle_s$ can be constructed from linear combination of $|k1\rangle$ and $|k2\rangle$ with appropriate complex coefficients A and B, so chosen such that $A|k1\rangle+B|k2\rangle=|k\rangle$ on the right (transmitted) side. Decomposition of $A|k1\rangle+B|k2\rangle$ as $(1/t)|k\rangle+(r/t)|-k\rangle$ on the left (incident) side yields the coefficients t and r. The procedure is exact within the tight-binding model. T is shown as a function of incident energy in Fig. 3. The energy bands for a perfect PPV is also shown. For the conduction ($D1^*$) and valence ($D1$) band, T raises sharply at the band edges. In fact, $T\sim k^2$ for cis-defect and carbonyl defect, while $T\sim k^4$ for sat-defect. T decreases after a maximum occurring near the energy with highest group velocity. Even higher values can be reached in other bands. The flat L and L^* bands are neglected because carriers are immobile in them. Symmetric features are found for $\pm\varepsilon$ for cis- and sat-defects. For cis-defect, $T=1/2$ when k is $0.073(\pi/a)$. The corresponding velocity is 1.75×10^5 m/s and kinetic energy is only 0.02 eV, implying the cis-defect cannot limit the carrier in a conjugation segment effectively. The situation for the sat-defect is

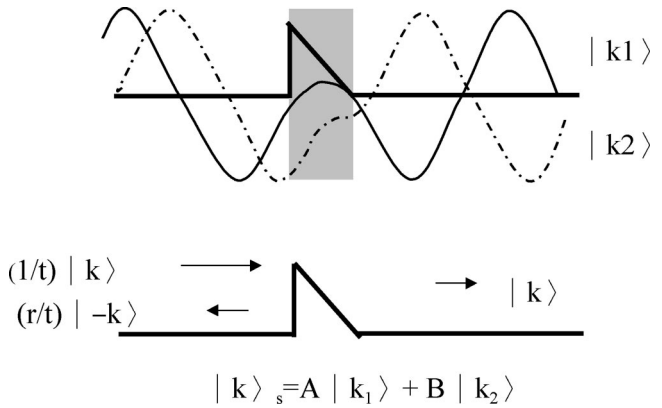

FIG. 2. The transmission amplitude t and reflection amplitude r are obtained from the phase shifts of the real solutions $|k1\rangle$ and $|k2\rangle$ across the defects. The picture is illustrated by the analogy with an one-dimensional triangular potential barrier.

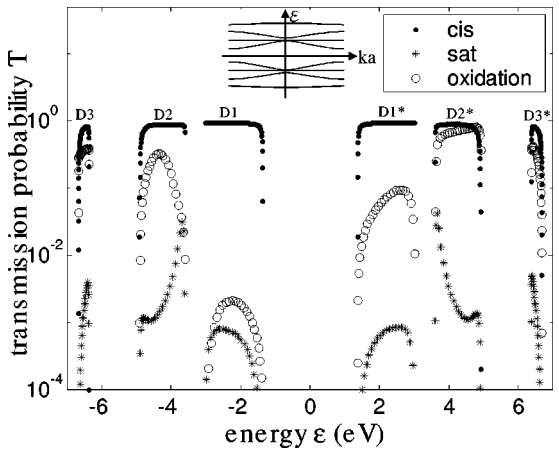

FIG. 3. The transmission probability T for the three conduction bands and three valance bands is shown as a function of incident electron energy.

completely different. T is less than 10^{-3} for the entire conduction and valence bands. So the carriers are strictly confined in the conjugation segments. The electron symmetry is broken for the carbonyl defect, for which the transport of the hole is strongly suppressed but the suppression for the electron is only moderate. Since holes are the main charge carriers,[9] the result is consistent with severe degradation of device performance by oxidation. T from the two incident directions are slightly different for the carbonyl defect. Only results for incidence from the left (refer to Fig. 1) are shown. This approach can be applied to interchain transition, in principle. Because the distance between the π orbitals is usually more separated in interchain case than in the sat-defect, the transmission probability is expected to be even lower. Phonon-assisted field tunneling is believed to be the main mechanism for interchain charge transport.

Below we apply the results on the transmission probability T to obtain the relation between drift velocity v_d and the electric field E. When a carrier travels in the perfectly conjugated segment between two defects, the drift velocity v_d^0 is determined by the phonon collisions. When the carrier hits the defect, it can either transmit or be reflected. If reflected, it will make a round trip and hit the same defect some time later, and so on (see Fig. 4). Eventually it will transmit after a time delay. Assuming the single round trip time is τ_r, the averaged time delay τ_d is

$$\tau_d = 0 + \tau_r(1-T)T + 2\tau_r(1-T)^2T + \cdots + n\tau_r(1-T)^nT + \cdots = \tau_r(1-T)/T. \quad (1)$$

The nth term corresponds to transmission after n attempts. The drift time τ_c within l_c is l_c/v_d^0. With the defect, the overall drift velocity v_d is equal to $l_c/(\tau_c+\tau_d)$. v_d^0 and τ_d depends strongly on the electric field, and have to be considered separately in the three field regimes. At low field, the carrier moves as a polaron, which is the combination of the carrier and the spontaneous lattice distortion around it.[15,16] The polaron saturates around the sound velocity v_s, so we take $v_d^0 = v_s$. The wave function of the carrier is a wave

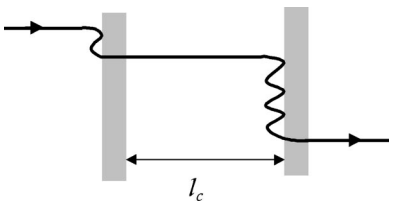

FIG. 4. The carrier hits the defect one or more times before transmitting through.

packet with the same group velocity v_g, defined by $v_g(k) = \partial\varepsilon(k)/\partial\hbar k$. $\varepsilon(k)$ is the energy band. The incident wave number k_i of the carrier upon the defect is so chosen such that $v_g(k_i) = v_s = 1.5\times10^4$ m/s.[17] $T(k_i)$ is used for T in Eq. (1). The round trip time τ_r in Eq. (1) for polaron has been determined by simulation on interchain hopping[16] to be 100 fs at $E = 10^7$ V/m. At other field τ_r is assumed to be inversely proportional to E. The reason is that during the round trip the polaron velocity is smaller than v_s and the lattice friction drops dramatically, so it moves like a free object obeying Newton's law. When E increases beyond E_1, polaron dissociates and the carrier becomes free. Within l_c, the carriers are accelerated by the field, then suffers collisions with phonons. Their transport properties are determined by the distribution function $f(k)$. In the intermediate regime, the carriers are still distributed near the band edge. The mean wave number $k^* = eE\tau_{ph}/\hbar$ is much smaller than the FBZ size π/a. τ_{ph} is the phonon collision time. Assuming a shifted Maxwell distribution with adjustable electron temperature T_e, $f(k)$, and v_d^0 can be obtained from the energy-balance condition $eEv_d^0 = \frac{1}{2}(T_e - T_l)k_B/\tau_{ph}$.[18] $T_l = 300$ K is the lattice temperature. τ_r is equal to τ_{ph} because of the predominance of back scattering with acoustic phonons.[19] The averaged value $T = \int T(k)f(k)dk$ after traveling over many conjugation segments should be used to obtain the delay time τ_d in Eq. (1).

In the intermediate regime, the drift velocity v_d^0 satisfies the balanced momentum and energy equations

$$mv_d^0 = eE\tau_{ph}, \quad eEv_d^0 = \frac{1}{2}k_B(T_e - T)\frac{1}{\tau_{ph}}. \quad (2)$$

m is the carrier effective mass. $\frac{1}{2}k_B(T_e - T)$ is the amount of energy dissipated from the electronic system to the lattice upon each emission of phonon. $\frac{1}{2}k_BT_e$ is the averaged initial electronic energy, and $\frac{1}{2}k_BT$ is the final electronic energy because the phonon emission tends to restore the system to equilibrium with the lattice at temperature T. Multiplying the above two equations we obtain $k_B(T_e - T) = 2(eE)^2\tau_{ph}^2/m$. The dissipated energy increases with E quadratically. The increasing dissipation power is crucial to balance the Joule heating eEv_d^0 as the field rises and maintain a stable $f(k)$ near the band edge. However, the dissipated energy cannot exceed the optical phonon energy $\hbar\omega_o = 0.17$ eV. Moreover, unlike the case of inorganic semiconductors, $\tau_{ph} = 10$ fs is almost independent of the carrier energy[19,20] because the density of state does not increase with energy. Consequently, the dissipation power saturates at $\hbar\omega_o/\tau_{ph}$ when the mean carrier energy $\frac{1}{2}T_ek_B$ is larger than $\hbar\omega_0$. Without an increas-

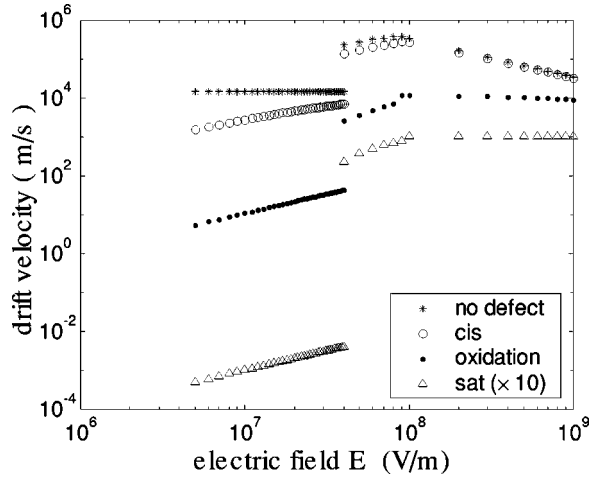

FIG. 5. The drift velocity is shown as a function of the electric field for three kinds of defects at the same density (one per 15 repeat units). The discontinuity at $E=4\times10^7$ V/m is due to polaron dissociation.

ing phonon emission rate to stabilize $f(k)$ around the band edge, the group velocity $v_g(k)$ of the carrier will blow up indefinitely as E further rises until it reaches the maximal group velocity determined by the band structure. Beyond the maximum, v_g starts to decrease and become negative after traveling half of the FBZ. Eventually $f(k)$ is stabilized by the finite bandwidth, and is expected to be very flat. The critical field E_2 is determined by $\frac{1}{2}T_e k_B=2\hbar\omega_0$. Beyond E_2, $f(k)$ simply approximated as a constant throughout the FBZ and we use $T=(a/\pi)\int_0^{\pi/a}T(k)dk$ for Eq. (1). From the modified energy-balance condition $eEv_d^0=\hbar\omega_0/\tau_{ph}$, v_d^0 is inversely proportional to E as

$$v_d^0=\frac{\hbar\omega_0}{eE\tau_{ph}} \quad E>E_2. \tag{3}$$

τ_r is determined by Bloch oscillation, which is now faster than the phonon back scattering. v_d^0 and v_d are shown as functions of E in Fig. 5. As E increases, the effect of the defects become weaker so v_d and v_d^0 are closer. The jump at $E_1=4\times10^7$ V/m is the signature of the polaron dissociation. Note the negative slope in the high-field regime due to Eq. (3). For cis-defects, the corresponding mobilty μ is about 10^{-4} m^2/Vs for polaron ($E<E_1$), and rise to about 10^{-3} m^2/Vs after polaron dissociation. Despite of the high conjugation defect density (1 per 15 repeat units), μ is six orders of magnitude larger then the bulk mobility (10^{-11} m^2/Vs),[9] 100 times larger then amorphous silicon ($10^{-6}\sim10^{-5}$ m^2/Vs),[21] and comparable to polycrystalline silicon ($10^{-4}\sim10^{-3}$ m^2/Vs).[21] Parallel charge transport is therefore a potential solution to the mobility problem in conjugated polymer devices. However, μ is 100 times smaller if the main conjugation defects are the carbonyl groups. For sat-defect, μ is it $5\sim7$ orders of magnitude smaller, so the transmission is practically negligible.

The cross sections for exciton gain and for polaron induced absorption are nearly equal in the spectral region where they overlap.[3] So net gain can be achieved only when the exciton density n_{ex} is higher than the polaron density n_p. Considering an active region with area A and thickness w sandwiched between two electrodes. In the steady state the exciton decay must be compensated by the current injection. So we have $Awn_{ex}/\tau_{ex}=An_p v_d$, where τ_{ex} is the exciton lifetime. The threshold condition $n_{ex}=n_p$ gives the critical drift velocity $v_c=w/\tau_{ex}$. Using $\tau_{ex}=0.3$ ns and $w=1$ μm, we get $v_c=3.3\times10^3$ m/s. This value can be achieved for intrachain transport with $E=10^7$ V/m. Assuming oxidation and sp^3 saturation can be avoided, PPV chains with average conjugation length equal to 100 Å and aligned over 1 μm are therefore expected to achieve net gain under parallel electric bias at 10 V.

In conclusion, the transmission probability for a carrier to tunnel through a variety of conjugation defects in conjugated polymers is calculated exactly within the tight-binding method for arbitrary incident energy. Contrary to the general belief, it is found that the typical conjugation defect (cis-defect) does not confine the carriers effectively. As a result, the effective mobility can be as high as 10^{-3} m^2/Vs for electric field above 4×10^7 V/m. It implies that the difficulties related to the low mobility can be eliminated, in principle, by better control over the chain alignment in solid state even with present level of conjugation defects.

This work was supported by the National Science Council of the Republic of China under Grant No. NSC89-2112-M009-047, the Excellence Project "Electroluminescence of Conjugated Polymers" of the ROC Ministry of Education, and Delta Electronics Inc.

*Corresponding author. Electronic address: meng@cc.nctu.edu.tw

[1] R. Friend, R. Gymer, A. Holmes, J. Burroughes, R. Marks, C. Taliani, D. Bradley, D. Dos Santos, J. Brédas, M. Lögdlund, and W. Salaneck, Nature (London) **397**, 121 (1999).
[2] M.D. McGehee and A.J. Heeger, Adv. Mater. **12**, 1655 (2000).
[3] N. Tessler, Adv. Mater. **11**, 363 (1999).
[4] K. Wong, M. Skaf, C.-Y. Yang, P.J. Rossky, B. Bagchi, D. Hu, J. Yu, and P.F. Barbara, J. Phys. Chem. B **105**, 6103 (2001).
[5] H.S. Woo, O. Lhost, S.C. Graham, D. Bradley, and R. Friend, Synth. Met. **59**, 29 (1993).
[6] S. Kishino, Y. Ueno, K. Ochiai, M. Rikukawa, K. Sanui, T. Kobayashi, H. Kunugita, and K. Ema, Phys. Rev. B **58**, R13 430 (1998).
[7] S. Kuroda, T. Noguchi, and T. Ohnishi, Phys. Rev. Lett. **72**, 286 (1994).
[8] E. Conwell, Phys. Rev. B **57**, R12 670 (1998).
[9] P. Blom and M. de Jong, IEEE J. Sel. Top. Quantum Electron. **4**, 105 (1998).
[10] H.-F. Meng and T.-M. Hong, Physica B **304**, 119 (2001).
[11] C. A. Coulson, B. O'Leary, and R. B. Mallion, *Hückel Theory for Organic Chemists* (Academic, London, 1978).
[12] R. Morrison and R. Boyd, *Organic Chemistry* (Allyn and Bacon, Boston, 1987).
[13] M. Rohlfing and S. Louie, Phys. Rev. Lett. **82**, 1959 (1999).
[14] V. F. Traven, *Frontier Orbitals and Properties of Organic Molecules* (Ellis Horwood, New York, 1992).

[15] S. Rakhmanova and E.M. Conwell, Appl. Phys. Lett. **75**, 1518 (1999).
[16] A. Johansson and S. Stafström, Phys. Rev. Lett. **86**, 3602 (2001).
[17] A.R. Bishop, D.K. Campbell, P.S. Lomdahl, B. Horovitz, and S.R. Phillpot, Phys. Rev. Lett. **52**, 671 (1984).
[18] K. Seeger, *Semiconductor Physics*, 2nd ed. (Springer-Verlag, Berlin, 1982).
[19] S. Jeyadev and E.M. Conwell, Phys. Rev. B **35**, 6253 (1987).
[20] E.M. Conwell, Phys. Rev. B **22**, 1761 (1980).
[21] *Polycrystalline and Amorphous Thin Films and Devices*, edited by L. Kazmerski (Academic, New York, 1980).